(Alternative) Analysis of COM-1094 data ("NIRISS Photometric Zeropoints", CAP-020)

Paul Goudfrooij, July 22, 2021
Updated: September 17, 2021

Simulated data files for flux standard stars P330E and WD1057+719 were copied from central store (/ifs/jwst/wit/niriss/cap_simulations/nis020) to local disk. For this analysis, I used the _rate.fits files. (The results were almost identical when using the _cal.fits files.)

The python scripts used in this analysis were run in a "clean" conda environment using python 3.9, to which packages `scipy, numpy, astropy, matplotlib, photutils, webbpsf`, and `pysynphot` were added using `pip install`. ***Note***: this presented one issue, namely that the `webbpsf` installation using `pip` also installs the `pysiaf` package, but since the latter is not supported through `pip` anymore as of version 0.12.0, *it installed version 0.11.0 instead which uses an old version of the SIAF*. To address this problem, I entered "`pip uninstall pysiaf`", then installed the latest version of `pysiaf` from GitHub through `git`, then changed directory to the top directory of the `pysiaf` installation, and finally entering "`pip install .`".

Since this dataset involves analysis of only one target (i.e., the flux standard star), I did not bother with establishing a source catalog. Instead, I just entered the expected pixel coordinates for the various pointings, using the SIAF information in conjunction with the dither tables. This was easy in this case, since all exposure specifications used the same 2-dither pattern. The scripts then used `photutils` functions to find the accurate centroids of the target.

Count Rate and Encircled Energy Measurements

First, I used script `getcircEE1.py` to obtain photometry and encircled energy (EE) data as follows:

```
python getcircEE1.py <input FITS file> <x> <y>
       <output flux table> <output EE table>
```

where <x> and <y> are the pixel coordinates of the source, estimated as mentioned above. The output of the `getcircEE1.py` script is as follows for each input FITS file:

1. Tabular output of relevant exposure parameters as well as the (max.) counts per integration in the central pixel of the target PSF (see Table A1 in the Appendix). **Note that several exposures are rather shallow and should be updated for the final flight version of the APT program.**
2. ASCII table with aperture photometry within various measurement radii. Currently, the source measurement radii are: [1,2,3,4,5,6,7,8,9,10,12,15], while the sky background is measured by default within an annulus of 5 pixels, the inner radius of which is 5 pixels outside the outermost source measurement radius (15 pixels in this case). The output

columns of this table consist of count rate measurements (both in ADU and in e^-) and their Poisson errors for each measurement radius, the (clipped mean) sky background level and its uncertainty, and the number of "good" pixels in the background annulus.

3. ASCII table with EE results, i.e., encircled integrated count rate as a function of measurement radius, along with their formal errors.

Script `getcircEE1.py` was run twice for each input FITS file: Once without any interpolation over bad pixels within the source aperture, and once with such interpolation activated. (See shell script do_photom1 for WD1057+719). The interpolation method used for this was borrowed from Kevin Volk's `image_interpolation.py` in the `niriss_commissioning` GitHub repo; specifically, I used the `fix_bad_pixels_surface` function which replaces the bad pixel's value by a 2-D surface fit to the surrounding area. However, I did not find any significant differences between the results of the two runs of `getcircEE1.py` for these data.

The results of the two dithers of each filter/subarray combination were combined and averaged using script `meanflux1.py`, which gathers all output EE files from `getcircEE1.py` for a given filter-subarray combination as input to this script. This script first identifies the radii for which each input EE table yields an integrated flux that is lower than that in the previous (smaller) radii; these measurements are flagged with zero weight. Then, it calculates weighted average fluxes at each radius, combining the fluxes measured at each dither step. (In the special case where all dithers have zero weight at a given measurement radius, a plain average is calculated.) The output of `meanflux1.py` is a table with average EE values and their uncertainties as function of measurement radius, along with a column that states the number of "good" (meaning non-zero-weight) measurements at that radius.

To establish reference aperture corrections for these measurements, I also created a set of WebbPSF images for each filter, using script `mkwebbPSFs.py`. These were 11-times oversampled PSFs, placed at the same pixel locations as the target star in these images, and then resampled back to the native pixel sampling. These WebbPSF images were rendered in relative flux units, where the total integrated flux is unity. For the WebbPSF images taken with the CLEARP element in the pupil wheel (i.e., images for filters with central wavelength > 2 μm), this involved a division by 0.84.

Before plotting the resulting EE values, the measured EE values for the simulated exposures of WD1057+719 and P330E were multiplied by the mean flux ratio "webbPSF/star", where that ratio was evaluated only at radii from 5 pixels to the outermost radius that was *not* flagged with zero weight (as described above). The resulting EE profiles from exposures with the subarrays SUB128 (for WD1057+719) and SUB80 (for P330E) are depicted in Figures 1 and 2 below.

Finally, the output EE tables from `meanflux1.py` were corrected for aperture corrections at the same measurement radii. To yield a final integrated count rate, I averaged the aperture-corrected values at radii of 5-8 pixels (see `totfluxes.py`). This avoids measurements at small radii which are sensitive to centering precision and focus variations, while also avoiding large radii for which flux measurements incur relatively large uncertainties, especially at low SNR (see

also Figure 1). The results for WD1057+719 and P330E are listed in Tables 2 and 4 below, respectively.

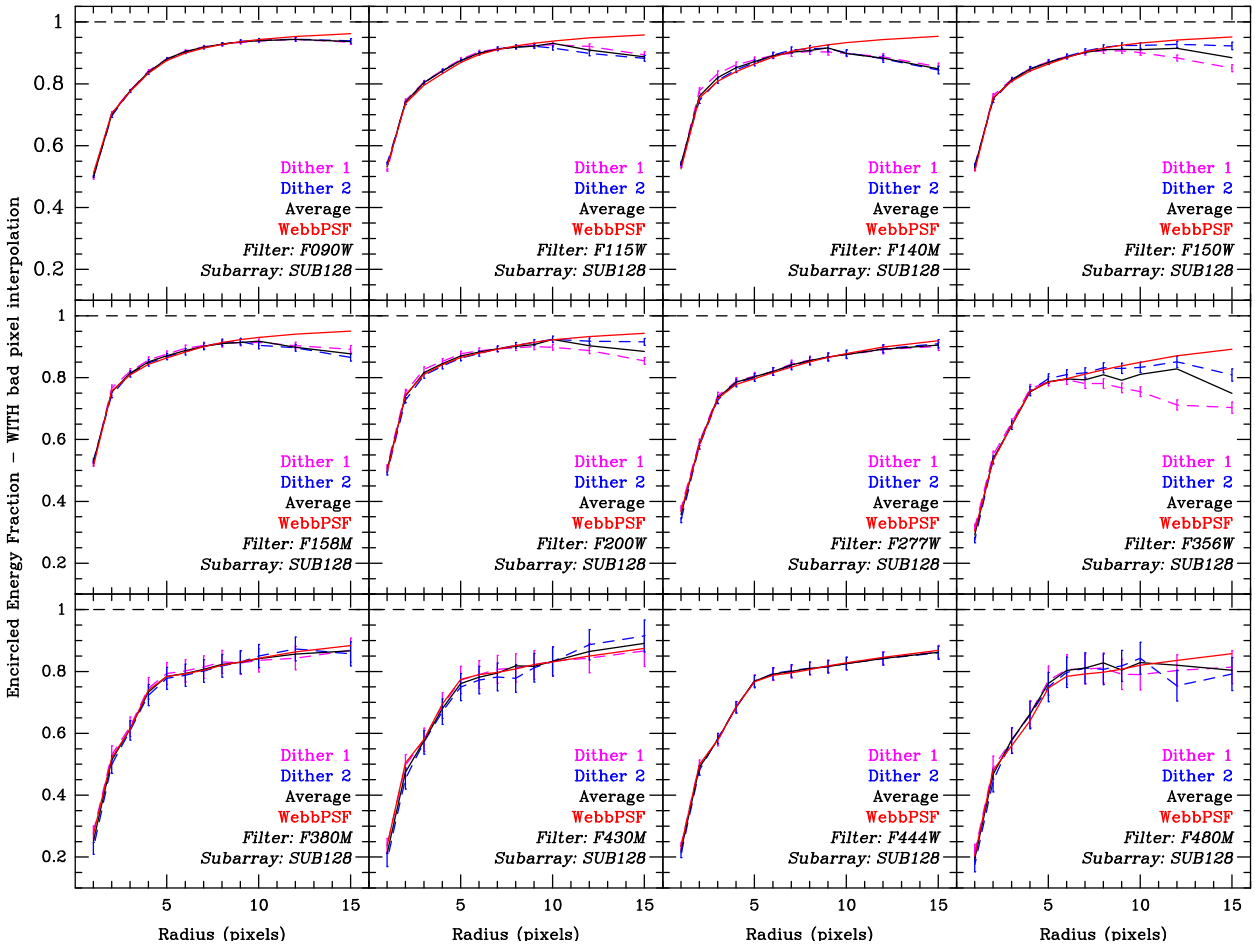

Figure 1: EE profiles for the simulated exposures of WD1057+719 with the SUB128 subarray, compared to the EE profiles of WebbPSF images. See legend for the meaning of the curves with different line colors. See text for details on how the EE values were evaluated.

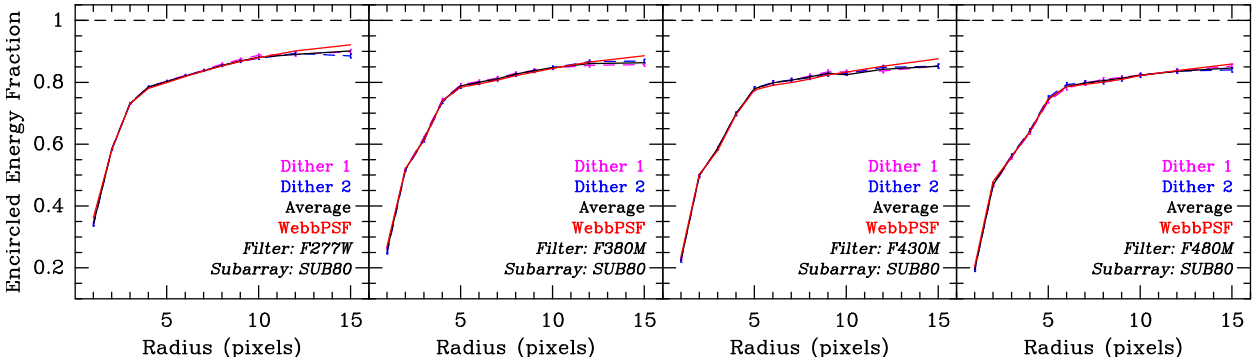

Figure 2: Same as Figure 1, but now for the simulated exposures of P330E with the SUB80 subarray and the CLEARP element in the pupil wheel.

Analysis of Outer Regions of EE Profiles

As seen in Figure 1, the EE profiles of some of the data for WD1057+719 show an unexpected downturn outside of a ~10 pix radius. These are most pronounced for the filters with central wavelength ≤ 2 μm and F356W, which have much shorter exposure times than the other filters (see Table A1 in the Appendix). To investigate the reason(s) for this downturn, I derived and plotted surface brightness (SB) profiles for the images in two ways: (1) straight measurements on the images (script getcircSB1.py), and (2) flagging pixels with values more than 3σ below the clipped mean sky value measured in a sky annulus outside a radius of 30 pixels, and excluding those flagged pixels from the SB measurements (script getcircSB2.py). The results are shown in Figure 3 below. Note that the inclusion (or exclusion) of the clipped low pixel values has a significant effect on the measured SB in the outer regions of the EE profiles for images with short exposure times. Note also that these clipped pixels are not flagged as 'bad' by the pipeline.

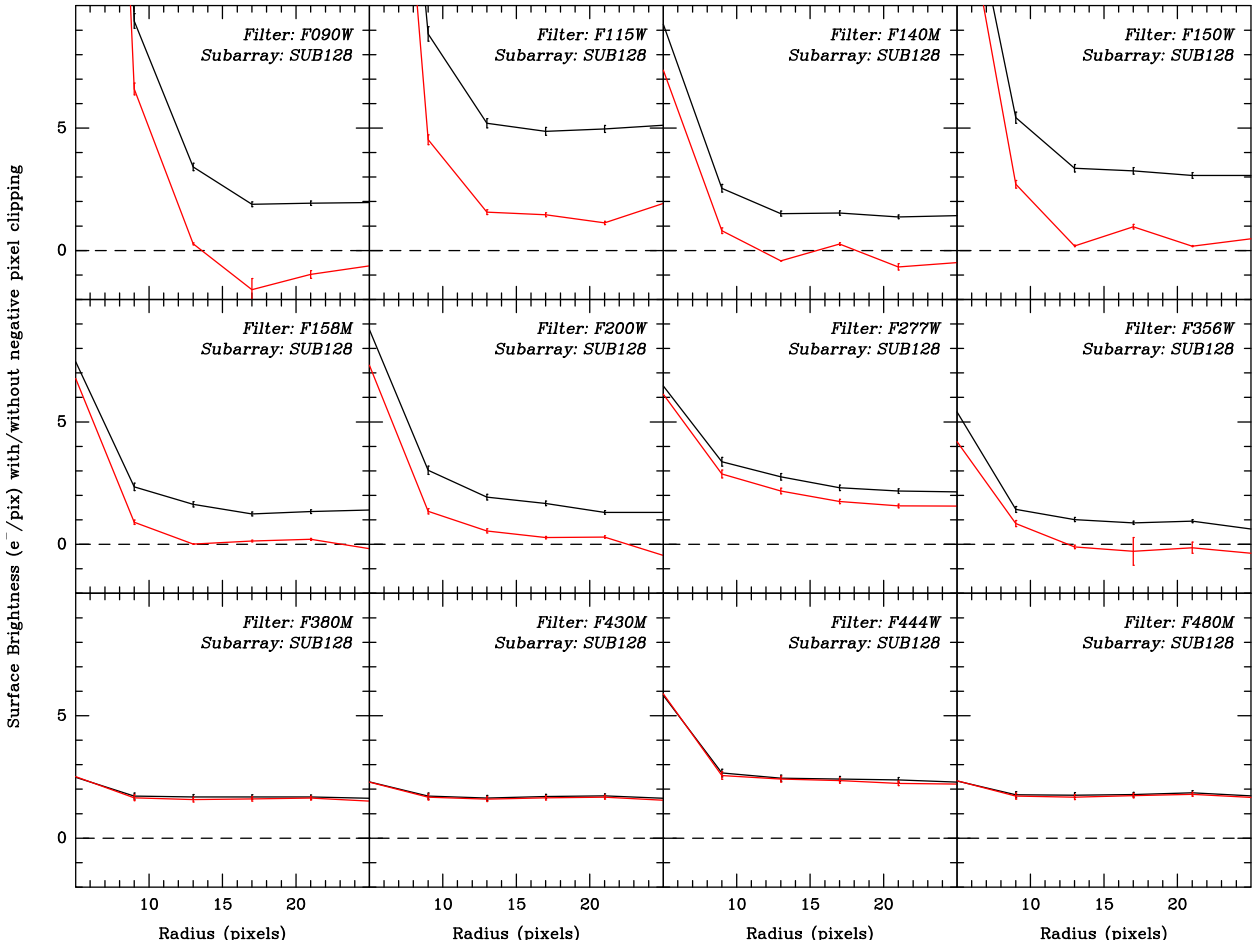

Figure 3: Surface brightness measurements on the SUB128 images of WD1057+719. Red lines represent straight measurements, while black lines represent measurements that exclude low pixel values that were clipped during the sky background measurements.

In Figure 4, I plot the result of running a version of getcircEE1.py in which the pixels within the radial limits of the EE profile with flagged low values identified above are replaced by those pixels in a median-filtered version of the image[1] prior to the photometry measurements. Note that this treatment fixes the downturn seen in the outer EE profiles in Figure 1 and renders EE profiles consistent with the WebbPSF ones to within the uncertainties.

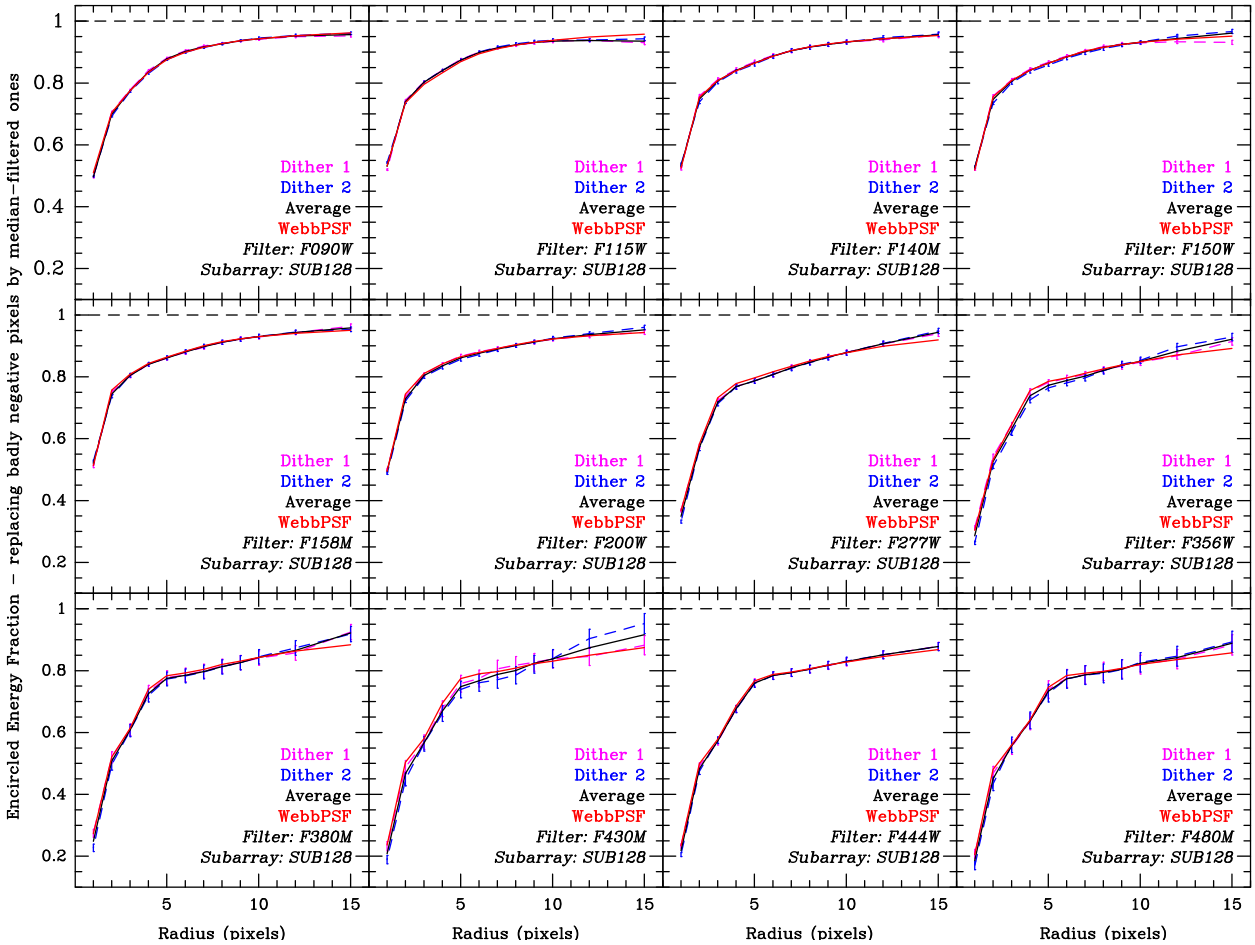

Figure 4: Same as Figure 1, but now showing measurements in which pixels with clipped low values are replaced by those pixels in a median-filtered version of the image prior to the photometry measurements.

Expected Count Rates

To compare the measured EE results with expectations for P330E and WD1057+719, we used a set of FITS files containing OTE and NIRISS throughputs as well as a "waveset" file (which defines a wavelength grid for interpolation purposes) that I put together for use with the Python `synphot` or `pysynphot` packages. This set of files is located on central store at `/ifs/jwst/wit/niriss/pysynphot`, along with a ReadMe file.

[1] The script (getcircEE1a.py) currently median filters a 40x40 pixel cutout around the source for this purpose.

The expected count rates for WD1057+719 and P330E were computed using `pysynphot`, using scripts `WD1057fluxes.py` and `P330Efluxes.py`, and listed below in Tables 3 and 5, respectively. I assumed a collection area of the JWST primary mirror of 254,009 cm^2, taken from the configuration files in the `Pandeia` package, and I assumed a detector gain of 1.6 e^-/ADU.

Table 2: Measured Count Rates for WD1057+719 in e^-/s, using Subarray = SUB128

F090W	F115W	F140M	F150W	F158M	F200W	F277W	F356W	F380M	F430M	F444W	F480M
0.87e+5	5.59e+4	1.64e+4	3.06e+4	1.40e+4	1.80e+4	0.88e+4	5.48e+3	1.01e+3	6.51e+2	3.31e+3	5.67e+2

Table 3: Expected Count Rates for WD1057+719 in e^-/s

F090W	F115W	F140M	F150W	F158M	F200W	F277W	F356W	F380M	F430M	F444W	F480M
1.03e+5	7.00e+4	2.03e+4	3.81e+4	1.76e+4	2.26e+4	1.32e+4	8.28e+3	1.49e+3	9.51e+2	4.98e+3	8.45e+2

Table 4: Measured Count Rates for P330E in e^-/s, using Subarray = SUB80

F277W	F380M	F430M	F480M
5.13e+5	6.15e+4	3.94e+4	3.47e+4

Table 5: Expected Count Rates for P330E in e^-/s

F277W	F380M	F430M	F480M
6.85e+5	8.21e+4	5.33e+4	4.72e+4

Conclusion

On average, I find that the measured count rates in the pipeline-processed simulated MIRAGE images are below the expected ones by ~20% for the PW filters, and by ~25% for the FW filters. The reason(s) for these discrepancies is/are currently unknown, and should probably be further investigated.

The short exposures among these simulated images suffer from strong background noise that affects the encircled energy measurements. I find that this can be addressed by replacing pixels with values lower than 3σ below the clipped mean sky value by those pixels in a median-filtered version of the image.

Appendix: Tables with exposure properties and maximum counts per integration

Table A1: Exposure properties of Observation 1 (WD1057+719)

Star: WD1057+719

Subarray: SUB64,	PW: F115W,	FW: CLEAR,	NGROUPS:	25,	NINTS:	5,	Max cnts/INT: 11704
Subarray: SUB64,	PW: F115W,	FW: CLEAR,	NGROUPS:	25,	NINTS:	5,	Max cnts/INT: 17921
Subarray: SUB64,	PW: F150W,	FW: CLEAR,	NGROUPS:	40,	NINTS:	5,	Max cnts/INT: 9660
Subarray: SUB64,	PW: F150W,	FW: CLEAR,	NGROUPS:	40,	NINTS:	5,	Max cnts/INT: 15119
Subarray: SUB64,	PW: F200W,	FW: CLEAR,	NGROUPS:	75,	NINTS:	5,	Max cnts/INT: 10124
Subarray: SUB64,	PW: F200W,	FW: CLEAR,	NGROUPS:	75,	NINTS:	5,	Max cnts/INT: 14573
Subarray: SUB128,	PW: F200W,	FW: CLEAR,	NGROUPS:	20,	NINTS:	3,	Max cnts/INT: 10104
Subarray: SUB128,	PW: F200W,	FW: CLEAR,	NGROUPS:	20,	NINTS:	3,	Max cnts/INT: 13294
Subarray: SUB128,	PW: F150W,	FW: CLEAR,	NGROUPS:	10,	NINTS:	3,	Max cnts/INT: 9204
Subarray: SUB128,	PW: F150W,	FW: CLEAR,	NGROUPS:	10,	NINTS:	3,	Max cnts/INT: 13404
Subarray: SUB128,	PW: F140M,	FW: CLEAR,	NGROUPS:	20,	NINTS:	3,	Max cnts/INT: 9978
Subarray: SUB128,	PW: F140M,	FW: CLEAR,	NGROUPS:	20,	NINTS:	3,	Max cnts/INT: 14868
Subarray: SUB128,	PW: F158M,	FW: CLEAR,	NGROUPS:	25,	NINTS:	3,	Max cnts/INT: 10332
Subarray: SUB128,	PW: F158M,	FW: CLEAR,	NGROUPS:	25,	NINTS:	3,	Max cnts/INT: 15037
Subarray: SUB128,	PW: F115W,	FW: CLEAR,	NGROUPS:	7,	NINTS:	3,	Max cnts/INT: 11810
Subarray: SUB128,	PW: F115W,	FW: CLEAR,	NGROUPS:	7,	NINTS:	3,	Max cnts/INT: 17789
Subarray: SUB128,	PW: F090W,	FW: CLEAR,	NGROUPS:	7,	NINTS:	3,	Max cnts/INT: 18417
Subarray: SUB128,	PW: F090W,	FW: CLEAR,	NGROUPS:	7,	NINTS:	3,	Max cnts/INT: 25191
Subarray: SUB128,	PW: CLEARP,	FW: F480M,	NGROUPS:	800,	NINTS:	2,	Max cnts/INT: 4944
Subarray: SUB128,	PW: CLEARP,	FW: F480M,	NGROUPS:	800,	NINTS:	2,	Max cnts/INT: 4516
Subarray: SUB128,	PW: CLEARP,	FW: F380M,	NGROUPS:	800,	NINTS:	2,	Max cnts/INT: 10393
Subarray: SUB128,	PW: CLEARP,	FW: F380M,	NGROUPS:	800,	NINTS:	2,	Max cnts/INT: 11297
Subarray: SUB128,	PW: CLEARP,	FW: F430M,	NGROUPS:	800,	NINTS:	2,	Max cnts/INT: 6037
Subarray: SUB128,	PW: CLEARP,	FW: F430M,	NGROUPS:	800,	NINTS:	2,	Max cnts/INT: 6074
Subarray: SUB128,	PW: CLEARP,	FW: F356W,	NGROUPS:	30,	NINTS:	3,	Max cnts/INT: 2553
Subarray: SUB128,	PW: CLEARP,	FW: F356W,	NGROUPS:	30,	NINTS:	3,	Max cnts/INT: 2685
Subarray: SUB128,	PW: CLEARP,	FW: F444W,	NGROUPS:	340,	NINTS:	3,	Max cnts/INT: 12042
Subarray: SUB128,	PW: CLEARP,	FW: F444W,	NGROUPS:	340,	NINTS:	3,	Max cnts/INT: 12607
Subarray: SUB128,	PW: CLEARP,	FW: F277W,	NGROUPS:	60,	NINTS:	3,	Max cnts/INT: 9952
Subarray: SUB128,	PW: CLEARP,	FW: F277W,	NGROUPS:	60,	NINTS:	3,	Max cnts/INT: 11745
Subarray: SUB256,	PW: CLEARP,	FW: F277W,	NGROUPS:	15,	NINTS:	3,	Max cnts/INT: 9714
Subarray: SUB256,	PW: CLEARP,	FW: F277W,	NGROUPS:	15,	NINTS:	3,	Max cnts/INT: 10991
Subarray: SUB256,	PW: CLEARP,	FW: F444W,	NGROUPS:	90,	NINTS:	3,	Max cnts/INT: 12278
Subarray: SUB256,	PW: CLEARP,	FW: F444W,	NGROUPS:	90,	NINTS:	3,	Max cnts/INT: 12515
Subarray: SUB256,	PW: CLEARP,	FW: F356W,	NGROUPS:	40,	NINTS:	3,	Max cnts/INT: 12326
Subarray: SUB256,	PW: CLEARP,	FW: F356W,	NGROUPS:	40,	NINTS:	3,	Max cnts/INT: 12956
Subarray: SUB256,	PW: CLEARP,	FW: F430M,	NGROUPS:	350,	NINTS:	2,	Max cnts/INT: 9588
Subarray: SUB256,	PW: CLEARP,	FW: F430M,	NGROUPS:	350,	NINTS:	2,	Max cnts/INT: 9654
Subarray: SUB256,	PW: CLEARP,	FW: F380M,	NGROUPS:	245,	NINTS:	2,	Max cnts/INT: 12467
Subarray: SUB256,	PW: CLEARP,	FW: F380M,	NGROUPS:	245,	NINTS:	2,	Max cnts/INT: 12772
Subarray: SUB256,	PW: CLEARP,	FW: F480M,	NGROUPS:	400,	NINTS:	2,	Max cnts/INT: 8311
Subarray: SUB256,	PW: CLEARP,	FW: F480M,	NGROUPS:	400,	NINTS:	2,	Max cnts/INT: 7980
Subarray: SUB256,	PW: F200W ,	FW: CLEAR,	NGROUPS:	6,	NINTS:	3,	Max cnts/INT: 11992
Subarray: SUB256,	PW: F200W ,	FW: CLEAR,	NGROUPS:	6,	NINTS:	3,	Max cnts/INT: 14935
Subarray: SUB256,	PW: F150W ,	FW: CLEAR,	NGROUPS:	4,	NINTS:	3,	Max cnts/INT: 14143
Subarray: SUB256,	PW: F150W ,	FW: CLEAR,	NGROUPS:	4,	NINTS:	3,	Max cnts/INT: 20225
Subarray: SUB256,	PW: F140M ,	FW: CLEAR,	NGROUPS:	6,	NINTS:	3,	Max cnts/INT: 11884
Subarray: SUB256,	PW: F140M ,	FW: CLEAR,	NGROUPS:	6,	NINTS:	3,	Max cnts/INT: 16948
Subarray: SUB256,	PW: F158M ,	FW: CLEAR,	NGROUPS:	7,	NINTS:	3,	Max cnts/INT: 11291
Subarray: SUB256,	PW: F158M ,	FW: CLEAR,	NGROUPS:	7,	NINTS:	3,	Max cnts/INT: 15667
Subarray: SUB256,	PW: F115W ,	FW: CLEAR,	NGROUPS:	3,	NINTS:	3,	Max cnts/INT: 20092
Subarray: SUB256,	PW: F115W ,	FW: CLEAR,	NGROUPS:	3,	NINTS:	3,	Max cnts/INT: 28439
Subarray: SUB256,	PW: F090W ,	FW: CLEAR,	NGROUPS:	3,	NINTS:	3,	Max cnts/INT: 30630
Subarray: SUB256,	PW: F090W ,	FW: CLEAR,	NGROUPS:	3,	NINTS:	3,	Max cnts/INT: 40461
Subarray: FULL ,	PW: CLEARP,	FW: F277W,	NGROUPS:	2,	NINTS:	2,	Max cnts/INT: 21948
Subarray: FULL ,	PW: CLEARP,	FW: F277W,	NGROUPS:	2,	NINTS:	2,	Max cnts/INT: 29170
Subarray: FULL ,	PW: CLEARP,	FW: F444W,	NGROUPS:	5,	NINTS:	2,	Max cnts/INT: 11636
Subarray: FULL ,	PW: CLEARP,	FW: F444W,	NGROUPS:	5,	NINTS:	2,	Max cnts/INT: 14060
Subarray: FULL ,	PW: CLEARP,	FW: F356W,	NGROUPS:	3,	NINTS:	2,	Max cnts/INT: 15489
Subarray: FULL ,	PW: CLEARP,	FW: F356W,	NGROUPS:	3,	NINTS:	2,	Max cnts/INT: 19080
Subarray: FULL ,	PW: CLEARP,	FW: F430M,	NGROUPS:	20,	NINTS:	1,	Max cnts/INT: 9104
Subarray: FULL ,	PW: CLEARP,	FW: F430M,	NGROUPS:	20,	NINTS:	1,	Max cnts/INT: 10815
Subarray: FULL ,	PW: CLEARP,	FW: F380M,	NGROUPS:	10,	NINTS:	2,	Max cnts/INT: 8401
Subarray: FULL ,	PW: CLEARP,	FW: F380M,	NGROUPS:	10,	NINTS:	2,	Max cnts/INT: 10286
Subarray: FULL ,	PW: CLEARP,	FW: F480M,	NGROUPS:	25,	NINTS:	1,	Max cnts/INT: 8571
Subarray: FULL ,	PW: CLEARP,	FW: F480M,	NGROUPS:	25,	NINTS:	1,	Max cnts/INT: 10134

Table A2: Exposure properties of Observation 2 (P330E)

Star: P330E

Subarray: SUB80 , PW: CLEARP, FW: F480M, NGROUPS: 100, NINTS: 3, Max cnts/INT: 12409
Subarray: SUB80 , PW: CLEARP, FW: F480M, NGROUPS: 100, NINTS: 3, Max cnts/INT: 13473
Subarray: SUB80 , PW: CLEARP, FW: F380M, NGROUPS: 35, NINTS: 3, Max cnts/INT: 10986
Subarray: SUB80 , PW: CLEARP, FW: F380M, NGROUPS: 35, NINTS: 3, Max cnts/INT: 12541
Subarray: SUB80 , PW: CLEARP, FW: F430M, NGROUPS: 70, NINTS: 3, Max cnts/INT: 11965
Subarray: SUB80 , PW: CLEARP, FW: F430M, NGROUPS: 70, NINTS: 3, Max cnts/INT: 13406
Subarray: SUB80 , PW: CLEARP, FW: F277W, NGROUPS: 3, NINTS: 3, Max cnts/INT: 11268
Subarray: SUB80 , PW: CLEARP, FW: F277W, NGROUPS: 3, NINTS: 3, Max cnts/INT: 14468

Subarray: SUB80 , PW: NRM   , FW: F277W, NGROUPS: 85, NINTS: 3, Max cnts/INT: 9191
Subarray: SUB80 , PW: NRM   , FW: F277W, NGROUPS: 85, NINTS: 3, Max cnts/INT: 13430
Subarray: SUB80 , PW: NRM   , FW: F430M, NGROUPS: 800, NINTS: 3, Max cnts/INT: 4231
Subarray: SUB80 , PW: NRM   , FW: F430M, NGROUPS: 800, NINTS: 3, Max cnts/INT: 5028
Subarray: SUB80 , PW: NRM   , FW: F380M, NGROUPS: 800, NINTS: 3, Max cnts/INT: 7606
Subarray: SUB80 , PW: NRM   , FW: F380M, NGROUPS: 800, NINTS: 3, Max cnts/INT: 9189
Subarray: SUB80 , PW: NRM   , FW: F480M, NGROUPS: 800, NINTS: 3, Max cnts/INT: 3112
Subarray: SUB80 , PW: NRM   , FW: F480M, NGROUPS: 800, NINTS: 3, Max cnts/INT: 3590
Subarray: SUB80 , PW: NRM   , FW: F480M, NGROUPS: 20, NINTS: 1, Max cnts/INT: 84
Subarray: SUB80 , PW: NRM   , FW: F480M, NGROUPS: 20, NINTS: 1, Max cnts/INT: 105